# Dramatic Changes in the Magnetic Coupling Mechanism for La-Doped $CaMnO_3$

E. Granado,[1,*] N. O. Moreno,[1] H. Martinho,[1] A. García,[1] J. A. Sanjurjo,[1,†] I. Torriani,[1] C. Rettori,[1] J. J. Neumeier,[2] and S. B. Oseroff[3]

[1]*Instituto de Física "Gleb Wataghin," UNICAMP, 13083-970, Campinas-SP, Brazil*
[2]*Department of Physics, Florida Atlantic University, Boca Raton, Florida 33431*
[3]*San Diego State University, San Diego, California 92182*

(Received 27 November 2000)

The exchange interactions in polycrystalline samples of $Ca_{1-x}La_xMnO_3$ ($0.00 \leq x \leq 0.05$) are studied by means of Raman scattering and electron paramagnetic resonance. Dramatic reductions in the spin-phonon interactions and magnetic correlations are observed for La doping levels as small as $\sim 2\%-3\%$. These results show that the charge carriers play an important role in the overall exchange coupling in the electron-doped manganites, even at very low doping levels.

DOI: 10.1103/PhysRevLett.86.5385 PACS numbers: 75.30.Vn, 63.20.–e, 76.30.–v, 78.30.–j

The exchange mechanisms involved in manganites have been a source of scientific interest for the last five decades. For this family of compounds, a competition between superexchange (SE) [1] and double-exchange (DE) [2] interactions has been widely accepted to explain the resulting spin alignment. Recently, the DE model was challenged by a calculation without adjustable parameters, indicating it may not be general enough to fully explain the ferromagnetism in doped manganites [3]. Thus, the development of microscopic probes, capable of identifying signatures of distinct exchange interaction mechanisms, are clearly needed to reveal the charge carrier role in the magnetic coupling.

The modulation of the exchange energy by specific zone-center lattice vibrations is responsible for a spin-phonon coupling, manifested by a renormalization of the involved phonon frequencies below the magnetic ordering temperature [4]. This effect is a fingerprint of the exchange mechanisms involved in a given magnetic material [5,6]. To obtain information about the nature of the exchange interactions involved in manganese perovskite systems, such as $Ca_{1-x}La_xMnO_3$, the simplest region of the phase diagram to be studied is for $x \lesssim 0.05$. This is because the number of $Mn^{3+}$ ions is small enough to prevent a complex orbital and/or charge ordering of $e_g$ electrons, but seems to be large enough to cause relevant changes in the magnetic and transport properties [7,8]. Also, previous studies in similar electron-doped $CaMnO_3$ systems reveal a number of unconventional physical properties [9–14]. In this work, we report temperature-dependent Raman-scattering and electron paramagnetic resonance (EPR) measurements in $Ca_{1-x}La_xMnO_3$ ($x = 0.00$, 0.02, 0.03, 0.05, 0.10, and 0.20), focusing on the spin-phonon coupling and antiferromagnetic (AFM) correlations in the low-concentration regime ($x \leq 0.05$). This combination of techniques shows unprecedented spectroscopic demonstrations of the strong impact of charge carriers on the magnetic coupling mechanisms in manganese perovskites.

The preparation of the polycrystalline samples used in this work was described previously [7]. Details of the x-ray [5], dc-magnetic susceptibility [5], and Raman-scattering [15] experiments are available in the literature. The EPR experiments were carried out in a Bruker $X$-band spectrometer, using a $TE_{102}$ room-temperature cavity and a helium gas flux (4–300 K) temperature controller.

Figure 1 shows unpolarized Raman spectra, at $T = 10$ K, of selected $Ca_{1-x}La_xMnO_3$ samples with $x = 0.00$, 0.02, 0.03, 0.05, 0.10, and 0.20. For $x = 0.00$, sharp peaks are observed that are tentatively classified according to the four general families of lattice vibrations Raman allowed for variants of the perovskite structure: external (Ca/La) modes, as well as rotational modes of the oxygen

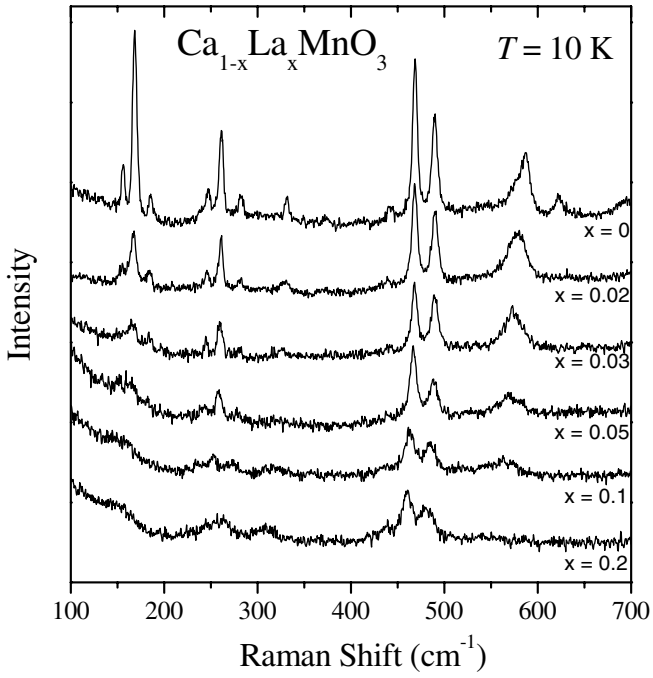


FIG. 1. Unpolarized Raman spectra at $T = 10$ K for $Ca_{1-x}La_xMnO_3$ with $0.00 \leq x \leq 0.20$.

  

octahedra in the lower-frequency region at 155, 170, 185, 245, 260, 280, and 330 $cm^{-1}$, bending vibrations of the octahedra at 445, 470, and 490 $cm^{-1}$, and an oxygen stretching mode at 585 $cm^{-1}$ (with a shoulder at $\sim$580 $cm^{-1}$). The peak at 625 $cm^{-1}$ is a spurious or defect mode, since it is only observed with the laser focused on specific regions of the sample. For $0.00 \leq x \leq 0.03$, a dramatic decrease of the Raman cross sections of the lowest-frequency modes at $T = 10$ K is observed (see Fig. 1). For $x \geq 0.03$, the stretching mode at $\sim$580 $cm^{-1}$ loses spectral weight and is not observed for $x > 0.10$. All the modes broaden as $x$ increases. These results are consistent with those previously published for $Ca_{1-x}La_xMnO_3$ ($x = 0.0$, 0.1, and 0.2) at room temperature [16,17].

The $T$ evolution of the Raman spectrum of $CaMnO_3$ in the region 420 $cm^{-1} \leq \omega \leq 630$ $cm^{-1}$ is shown in Fig. 2. Figure 3(a) shows the $T$ dependence of the 470, 490, and 585 $cm^{-1}$ phonon frequencies. It is clear from Figs. 2 and 3(a) that anomalous softenings of the oxygen bending modes and hardening of the stretching mode take place at $T \lesssim 130$ K $\sim T_N$ [7]. A small softening of the 260 $cm^{-1}$ mode below $T_N$ was also detected (not shown). No frequency anomaly was observed for the 170 $cm^{-1}$ mode. Also, no anomaly at $T_N$ on the peak linewidths was observed for any of the studied modes, within our experimental resolution. The $T$ dependence of the orthorhombic **a**, $\mathbf{b}/\sqrt{2}$, and **c** lattice parameters (*Pnma* space group), and the unit cell volume, **V**, are displayed in Fig. 3(b) for the undoped sample. Notice that lattice anomalies due to magneto and/or exchange strictive effects are very small in $CaMnO_3$, although slight changes in **a** and **V** are noticed below $T_N$. This compound shows a quasicubic perovskite structure, reflecting the nearly identical $Mn^{4+}(3t_{2g})$-$O(2p)$ bonds for the three binding directions. Therefore, the Grüneisen law, $\Delta\omega/\omega = -\gamma\Delta\mathbf{V}/\mathbf{V}$, is a good approximation for the lattice contribution to the frequency shifts. This term is estimated in Fig. 3(a) as solid lines, using the data shown in Fig. 3(b). Figures 3(a) and 3(b) show that the softening and hardening effects on the phonon frequencies at the AFM transition cannot be ascribed to lattice anomalies. This is also realized from the fact that the frequency shifts of bending and stretching modes have opposite signs. Finally, no renormalization of electronic states, that could justify phonon frequency shifts, occurs at $T_N$ [7]. The above considerations led us to conclude that the phonon frequency anomalies below $T_N$ in $CaMnO_3$ [see Figs. 2 and 3(a)] are due to spin-phonon coupling.

To our present knowledge, two possible physical mechanisms may lead to measurable frequency shifts due to

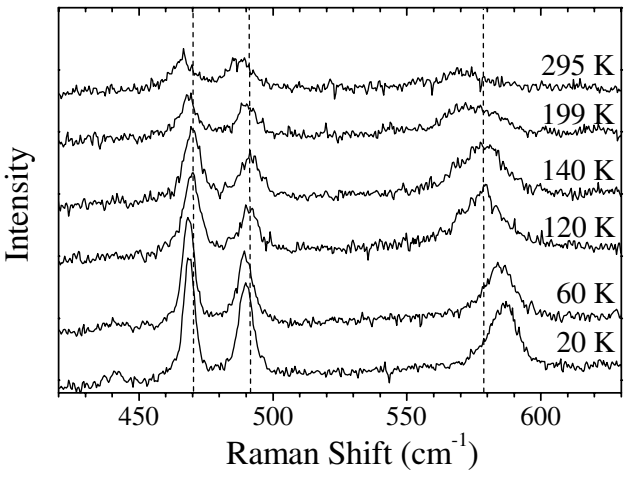


FIG. 2. $T$ dependence of the unpolarized Raman spectrum of $CaMnO_3$.

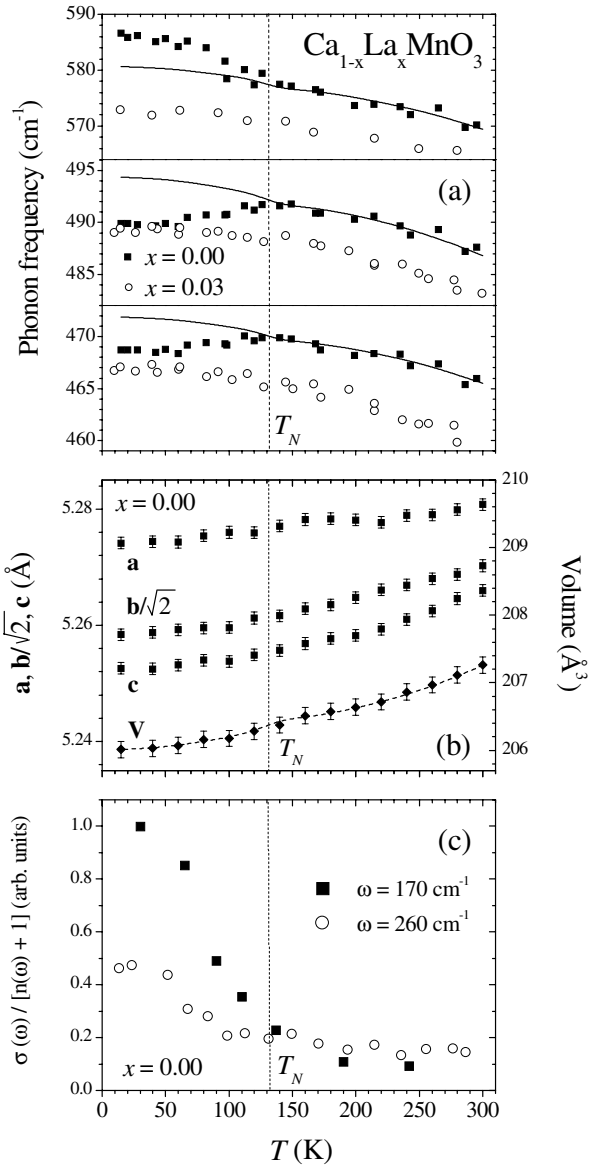


FIG. 3. $T$ dependence of (a) the phonon frequency for the two bending modes ($\sim$470 and $\sim$490 $cm^{-1}$) and the stretching mode ($\sim$585 $cm^{-1}$) for $Ca_{1-x}La_xMnO_3$ with $x = 0.00$ and 0.03; (b) the lattice parameters and the unit cell volume for $CaMnO_3$; and (c) the intensity of the low-frequency modes at $\sim$170 and $\sim$260 $cm^{-1}$ for $x = 0.00$. The solid lines in (a) are the expected behavior for the phonon frequencies according to the Grüneisen law, $\Delta\omega/\omega = -\gamma\Delta\mathbf{V}/\mathbf{V}$, using the data shown in (b).

spin-phonon effects. They arise from the coupling of the magnetic energy with the ionic displacements in first order in a nonadiabatic regime [18], or in second order [4]. However, the former mechanism is not active in the present case, since it would lead to strong lattice anomalies at $T_N$ that were not observed [see Fig. 3(b)]. Notice that the frequency anomalies are observed in vibrations of oxygen ions, rather than magnetic $Mn^{4+}$ ions. On the other hand, the second mechanism above can quite naturally explain the phonon anomalies observed in $CaMnO_3$ [4].

The $T$ dependence of the bending and stretching mode frequencies observed in $Ca_{0.97}La_{0.03}MnO_3$ is shown in Fig. 3(a). The anomalous frequency shifts detected in $CaMnO_3$ are not observed for a La doping of 3%, implying a dramatic weakening of the spin-phonon coupling. Since both compounds show very similar sets of lattice parameters (apart from a small isotropic expansion of $\sim 0.2\%$ for $x = 0.03$), this result is a strong evidence that very weak electron doping of $CaMnO_3$ causes the magnetic coupling mechanism between Mn ions to change dramatically. Spin-phonon coupling by oxygen vibrations is a usual feature of SE systems; the suppression of this effect for $Ca_{0.97}La_{0.03}MnO_3$ suggests an overall exchange coupling which is much weaker and/or less dependent on oxygen ion positions. $Ca_{1-x}La_xMnO_3$ samples with $x = 0.005$, 0.01, and 0.02 were also studied (not shown), with frequency anomalies still being observed for these compositions. Finally, no frequency shifts at the magnetic ordering temperature were observed for $x = 0.07$.

Figure 3(c) displays the $T$ dependence of the Raman cross sections of the most intense low-frequency modes ($\sim 170$ and $\sim 260\ cm^{-1}$) for the $x = 0.00$ sample. A strong enhancement of the $\sim 170\ cm^{-1}$ line, as well as a weaker effect for the $\sim 260\ cm^{-1}$ mode, is observed at $T \lesssim T_N$. Enhancement effects on Raman cross sections were not observed for the $x = 0.03$ sample. Notice that the intensity of the $\sim 170\ cm^{-1}$ mode remains quite small even at low temperatures for this doped sample (see Fig. 1). We should mention that the modes at 155, 280, 330, 470, and $490\ cm^{-1}$ also show detectable intensity increases below $T_N$ for the undoped sample (not displayed).

Changes of Raman cross section of vibrational modes near the magnetic ordering temperature are commonly interpreted in the framework introduced by Suzuki and Kamimura [19]. According to this theory, one of the possible mechanisms which may give rise to a spin dependent polarizability in insulators is the variation of nondiagonal exchange with the relative displacements of ions. Thus, the observation of spin dependent Raman cross sections for $CaMnO_3$, and the suppression of this effect for the $x = 0.03$ sample also supports dramatic changes in the magnetic coupling mechanism on $CaMnO_3$ with doping.

In order to gain further insight into the nature of the magnetic interactions present in this system, we have also performed EPR measurements. Figure 4 shows, for $T \gtrsim T_N$, the $T$ dependence of the EPR linewidth, $\Delta H$, for the $[(1 - x)Mn^{4+} + xMn^{3+}]$ spin coupled system in the $Ca_{1-x}La_xMnO_3$ samples with $x = 0.00$, 0.02, and 0.05. A single resonance with a $T$ independent $g \approx 2.00(9)$ value and a dysonian line shape [20] was observed for all the samples. Notice the large difference between the $\Delta H$ vs $T$ for the undoped and doped compounds. For $CaMnO_3$, unlike $LaMnO_3$ [17], $\Delta H$ is $T$ dependent and smoothly decreases up to temperatures well above $T_N$. This behavior is similar to that found in the paramagnetic phase of systems exhibiting spin-freezing phenomenon at low $T$ (spin glasses), and can be understood as a manifestation of the presence of short-range magnetic correlations at $T \gg T_N$. Figure 4 shows the fitting of $\Delta H$ to $\Delta H(\infty) + A \exp[-(T - T_N)/T_0]$ for the $x = 0.00$ sample, where $\Delta H(\infty)$ is the high-$T$ linewidth, and $A$ and $T_0$ are empirical parameters associated to the spin freezing [21]. For the doped samples the $T$ dependence of $\Delta H$ is very different. For $T$ not much larger than $T_N$, $\Delta H$ becomes $T$ independent, and as $T$ approaches $T_N$ from above, a sharp line broadening and small resonance shift (not shown) are observed. The linewidth for the doped samples could not be fitted by the exponential law used for the undoped sample. Instead, Fig. 4 shows the fitting of $\Delta H$ by a power law, $\Delta H = \Delta H(\infty) + A/(T - T_N)^{\beta}$ for the $x = 0.05$ sample. This expression was previously used to account for critical short-range correlations in AFM materials above $T_N$ [22]. Intriguingly, the data for undoped and lightly doped samples could not be fit by the same expression. It is apparent that the exponential law accounts better for systems with strong magnetic correlations well above $T_N$, while the materials presenting only critical correlations near $T_N$ are better described by the power law. Overall, the basically $T$ independent $\Delta H$ above $T_N$ for the $x = 0.02$

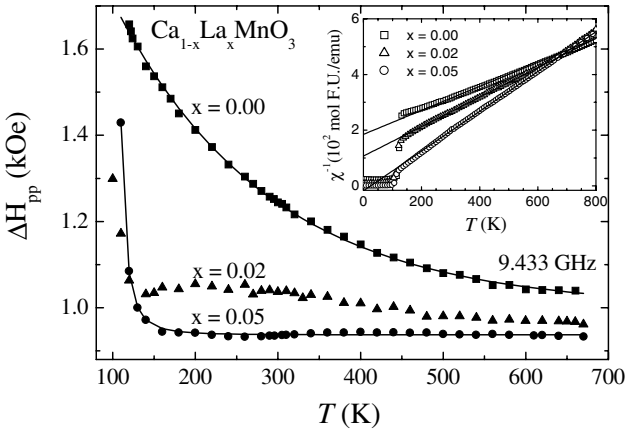


FIG. 4. $T$ dependence of the EPR linewidth in $Ca_{1-x}La_xMnO_3$ samples ($x = 0.00, 0.02, 0.05$). The solid lines are fittings to $\Delta H_{pp} = \Delta H_{pp}(\infty) + Ae^{-(T-T_N)/T_0}$ for $x = 0$ [$\Delta H_{pp}(\infty) = 1$ kOe, $A = 666$ kOe, $T_N = 112$ K, $T_0 = 186$ K] and $\Delta H_{pp} = \Delta H_{pp}(\infty) + A/(T - T_N)^{\beta}$ for $x = 0.05$ [$\Delta H_{pp}(\infty) = 0.9$ kOe, $A = 3.4$ kOe K, $\beta = 2.4$, and $T_N = 95$ K]. The inset shows $\chi^{-1}(T) = (T - \Theta)/C$. The Curie-Weiss fitting parameters are $\Theta = -429$ K, $p_{\text{eff}} = 4.31\mu_B$ ($x = 0.00$); $\Theta = -202$ K, $p_{\text{eff}} = 3.89\mu_B$ ($x = 0.02$); and $\Theta = 25$ K, $p_{\text{eff}} = 3.35\mu_B$ ($x = 0.05$).

and $x = 0.05$ samples shows that the magnetic correlations at high $T$ observed in the parent compound are dramatically reduced by electron doping. Notice that $\Delta H(\infty)$ remains about the same ($\sim$1000 Oe) for all the studied samples, suggesting that antisymmetric interactions contributing to $\Delta H$ are not seriously affected by doping [23]. The inset of Fig. 4 shows the paramagnetic susceptibility for the same samples measured by EPR. The large negative Curie-Weiss temperature of $CaMnO_3$ ($\Theta = -429$ K) indicates a strong AFM coupling between $Mn^{4+}$ spins, and is consistent to the observation of magnetic correlations at high $T$ by EPR. We should mention that the relatively small value of $T_N = 130$ K is likely due to unusually strong AFM second neighbor interactions [14], which are frustrated in the AFM ordered phase. As was reported earlier, the value of $\Theta$ is dramatically increased by electron doping [8,10,11,14], in agreement with the conclusions derived from the EPR data.

In conclusion, our Raman scattering and EPR results give compelling evidence that only a small level ($\sim$2%–3%) of $La^{3+}$ electron doping in $Ca_{1-x}La_xMnO_3$ is enough to change dramatically the overall exchange coupling between the Mn ions, both in the ordered ($T \lesssim T_N$) and disordered ($T \gtrsim T_N$) phases. These results give strong support to the widely accepted notion that the charge carriers play a decisive role in the exchange coupling in manganese perovskites. It is surprising, though, that dramatic effects were observed at such small doping levels. For $x = 0.03$, for example, the fraction of $Mn^{3+}O^{2-}Mn^{4+}$ bonds is only $\sim$6%, and therefore signatures of the dominant $Mn^{4+}O^{2-}Mn^{4+}$ SE interactions ($\sim$94% of bonds) might be present in our spectroscopic measurements. More importantly, the small saturation magnetization ($M_S$) observed for $x = 0.03$ ($\sim 0.1\mu_B$/Mn ion) indicates that the Mn $3t_{2g}$ core electrons are still antiferromagnetically ordered in the lattice at low $T$ [7], with only a small canting of $\sim 2^\circ$ (mean field scenario) or a small volume fraction of FM domains ($\sim$3%, phase separation scenario). In this context, our results show that the overall exchange interactions are strongly affected by the doping electrons, both in the AFM and in the paramagnetic phases. In fact, our combined Raman, EPR, and susceptibility results indicate that the exchange between core $Mn^{4+}$ spins evolves from strong and long-range AFM coupling in $CaMnO_3$ to a much weaker AFM overall exchange interaction for electron doping levels of only $\sim$2%–3%. This clear distinction between the influence of charge carriers on the exchange interactions and their influence on $M_S$ itself is inconsistent with the original DE model [2], and therefore additional mechanisms may be necessary to account for the dramatic weakening of the AFM interactions for $0 \leq x \lesssim 0.03$. Recent calculations indicated competition among lattice and spin polarons for electron-doped $CaMnO_3$ [24]. A critical doping level of $x = 0.045$ was predicted, where the polarons are unstable relative to an undistorted FM ground state. Interestingly, for $x \gtrsim 0.02$ and $T \sim T_N$, our EPR data may be perceived as a rapid decrease of the magnetic correlation length with increasing $T$ (see Fig. 4), suggesting a reduction of polaron size at $T_N$. Besides, at $x \gtrsim 0.02$–$0.03$, spin-phonon coupling effects disappear [see Fig. 3(a)], $\Delta H$ becomes basically $x$ and $T$ independent at $T > T_N$ (see Fig. 4), and $M_S$ starts to increase considerably [7]. These results may suggest the existence of two doping regimes with quite distinct behaviors. Finally, this study shows that spin-phonon coupling effects can be used as a unique and powerful microscopic probe to investigate exchange interactions in complex magnetic materials.

This work was supported by FAPESP, CNPq (Brazil), and NSF (U.S.A).

*Present address: NCNR, NIST, Gaithersburg, MD 20874, and CSR, Department of Physics, University of Maryland, College Park, MD 20742.
†Deceased.

[1] J. B. Goodenough, *Magnetism and the Chemical Bound* (John Wiley, New York, 1963).
[2] C. Zener, Phys. Rev. **82**, 403 (1951); P. W. Anderson and H. Hasegawa, Phys. Rev. **100**, 675 (1955); P.-G. de Gennes, Phys. Rev. **118**, 141 (1961).
[3] G.-m. Zhao, Phys. Rev. B **62**, 11 639 (2000).
[4] W. Baltensperger and J. S. Helman, Helv. Phys. Acta **41**, 668 (1968).
[5] E. Granado *et al.,* Phys. Rev. B **60**, 11 879 (1999).
[6] E. Granado *et al.,* Phys. Rev. B **60**, 6513 (1999).
[7] J. J. Neumeier and J. L. Cohn, Phys. Rev. B **61**, 14 319 (2000).
[8] J. J. Neumeier and D. H. Goodwin, J. Appl. Phys. **85**, 5591 (1999).
[9] V. A. Bokov *et al.,* Phys. Status Solidi **20**, 745 (1967); W. Bao *et al.,* Phys. Rev. Lett. **78**, 543 (1997); C. Martin *et al.,* J. Solid State Chem. **134**, 198 (1997); I. O. Troyanchuk *et al.,* J. Solid State Chem. **131**, 144 (1997); R. Mahendiran *et al.,* Phys. Rev. B **62**, 11 644 (2000); M. M. Savosta *et al.,* Phys. Rev. B **62**, 9532 (2000).
[10] H. Chiba *et al.,* Solid State Commun. **99**, 499 (1996).
[11] A. Maignan *et al.,* Phys. Rev. B **58**, 2758 (1998).
[12] A. Maignan *et al.,* Chem Mater. **10**, 950 (1998).
[13] C. Martin *et al.,* Phys. Rev. B **62**, 6442 (2000).
[14] H. Aliaga *et al.,* e-print cond-mat/0010295.
[15] E. Granado *et al.,* Phys. Rev. B **62**, 11 304 (2000).
[16] E. Liarokapis *et al.,* Phys. Rev. B **60**, 12 758 (1999).
[17] E. Granado *et al.,* Phys. Rev. B **58**, 11 435 (1998).
[18] G. Wellein *et al.,* Phys. Rev. Lett. **81**, 3956 (1998).
[19] N. Suzuki and H. Kamimura, J. Appl. Phys. **35**, 985 (1973).
[20] G. E. Pake and E. M. Purcell, Phys. Rev. **74**, 1184 (1948).
[21] S. M Bhagat *et al.,* Solid State Commun. **38**, 261 (1981).
[22] D. L. Huber, Phys. Rev. B **6**, 3180 (1972); S. B. Oseroff, Phys. Rev. B **25**, 6584 (1982).
[23] D. L. Huber *et al.,* Phys. Rev. B **60**, 12 155 (1999).
[24] Y.-R. Chen and P. B. Allen, e-print cond-mat/0101354.